Running head: No elevated CO_2 impact on woodland water-use

Elevated CO_2 did not affect the hydrological balance of a mature native *Eucalyptus* woodland

Teresa E. Gimeno [1,2,3*], Tim R. McVicar [4,5], Anthony P. OʼGrady [6], David T. Tissue [2] and David S. Ellsworth [2]

[1] INRA, UMR ISPA, F-33140, Villenave dʼOrnon, France

[2] Hawkesbury Institute for the Environment, Western Sydney University, Penrith, NSW 2751, Australia

[3] *Present address*: Basque Centre for Climate Change (BC3), 48940, Leioa, Spain

[4] CSIRO Land and Water, GPO Box 1700, Acton, Canberra ACT 2601, Australia

[5] Australian Research Council Centre of Excellence for Climate System Science, Sydney, NSW Australia

[6] CSIRO Land and Water, Private Bag 12, Hobart, TAS 7001, Australia

[*] Corresponding author:
Teresa E. Gimeno
E-mail: teresa.gimeno@inra.fr
Phone: +33 (0) 5 57 12 27 63

Paper type: Primary Research Article

Originally submitted to *Global Change Biology* on 23 November 2017. Manuscript provisionally accepted with minor revisions on 13 February 2018. Revised version submitted on 12 March 2018

Keywords: climate change, *Eucalyptus tereticornis*, FACE, interception, tree water, stomatal conductance, water use efficiency.

ABSTRACT

Elevated atmospheric CO_2 concentration (eC_a) might reduce forest water-use, due to decreased transpiration, following partial stomatal closure, thus enhancing water-use efficiency and productivity at low water availability. If evapotranspiration (E_t) is reduced, it may subsequently increase soil water storage (φS) or surface runoff (R) and drainage (D_g), although these could be offset or even reversed by changes in vegetation structure, mainly increased leaf area index (L). To understand the effect of eC_a in a water-limited ecosystem, we tested whether two years of eC_a (~40% increase) affected the hydrological partitioning in a mature water-limited *Eucalyptus* woodland exposed to Free-Air CO_2 Enrichment (FACE). This timeframe allowed us to evaluate whether physiological effects of eC_a reduced stand water-use irrespective of L, which was unaffected by eC_a in this timeframe. We hypothesized that eC_a would reduce tree-canopy transpiration (E_{tree}), but excess water from reduced E_{tree} would be lost via increased soil evaporation and understory transpiration (E_{floor}) with no increase in φS, R or D_g. We computed E_t, φS, R and D_g from measurements of sapflow velocity, L, soil-water content (θ), understory micro-meteorology, throughfall and stemflow. We found that eC_a did not affect E_{tree}, E_{floor}, φS or θ at any depth (to 4.5 m) over the experimental period. We closed the water balance for dry seasons with no differences in the partitioning to R and D_g between C_a levels. Soil temperature and θ were the main drivers of E_{floor} while vapour pressure deficit controlled E_{tree}, though eC_a did not significantly affect any of these relationships. Our results suggest that in the short-term, eC_a does not significantly affect ecosystem water-use at this site. We conclude that water-savings under eC_a mediated by either direct effects on plant transpiration or by indirect effects via changes in L or soil moisture availability are unlikely in water-limited mature eucalypt woodlands.

Introduction

Rising atmospheric CO_2 concentration (C_a) directly affects several facets of plant physiology, with cascading effects on other biotic and abiotic ecosystem components (Field *et al.*, 1995). At the leaf-level, increases in C_a above the present concentration often enhance photosynthesis, reduce transpiration, due to partially reduced stomatal conductance (g_s), and thus increase water-use efficiency (De Kauwe *et al.*, 2013, Keenan *et al.*, 2013), though the ecosystem-level ramifications of these effects are still debated (Leuzinger & Körner, 2010, Donohue *et al.* 2017). In vegetated areas, evapotranspiration is a major contributor to ecosystem water balance (Zhang *et al.*, 2016). At steady-state conditions, reduced transpiration under elevated C_a (eC_a) may lead to increased soil moisture (Leuzinger & Körner, 2007) and eventually an increase in the amount of precipitation running off the ground surface (R) and into groundwater stores (D_g, Gedney *et al.*, 2006, Zhang *et al.*, 2001). Numerous modelling studies and retrospective analyses have ascribed observed increases in R or soil water storage (φS) to rising C_a (Aston, 1984, Betts *et al.*, 2007, Jackson *et al.*, 1998, Macinnis-Ng et al., 2011). Yet, more recent studies highlight that these observations are strongly dependent on the vegetation type and climate (Cheng *et al.*, 2014, Fatichi *et al.*, 2016, Huntington, 2008, Leuzinger & Körner, 2010). However, these predictions rely mostly on retrospective analyses encompassing the increase in C_a from pre-industrial to current C_a levels (Betts *et al.*, 2007, Gedney *et al.*, 2006, Ukkola *et al.*, 2016) and these might not necessary apply to further projected increases in C_a for the 21st century.

Rising C_a also affects transpiration indirectly (Fatichi *et al.*, 2016), as enhanced total or above-ground productivity would require more water to support more tissue produced in eC_a (Ellsworth *et al.*, 2012, Norby *et al.*, 2005). Satellite observations and model predictions indicate that rising C_a partly underlies the recent global increase in woody biomass and greenness (Zhu *et al.*, 2016), particularly in water-limited regions (Donohue *et al.*, 2009). Increased greenness due to present-day CO_2-fertilization results from greater leaf area per unit of ground area (*L*, McCarthy *et al.*, 2007, Cheng *et al.*, 2017), which increases transpiration surface area per unit of ground area (Macinnis-Ng *et al.*, 2011). Such an effect may offset or even override potential leaf-level reductions in transpiration. Additionally, increased radiative forcing due to climate change would further offset the potential impacts of reduced stomatal conductance under eC_a (Ukkola *et al.*, 2016, Cheng *et al.* 2014). Indeed, under eC_a, Donohue *et al.* (2017) predict no effective ecosystem-level water-savings in either water-limited sites, where increased *L* offsets leaf-level water-savings, or in so-called ﾓenergy-limitedﾔ sites (cf. Zhang *et al.*, 2001), where little or no change of leaf-level transpiration is expected and where *L* is already maximised (Yang *et al.*, 2016b). Alternatively, in sub-humid and semi-arid river basins, increased greenness due to eC_a could increase ecosystem-level water-use and reduce streamflow (Trancoso *et al.*, 2017, Ukkola *et al.*, 2016).

In addition to the impact on transpiration, increased *L* indirectly alters ecosystem water-use by increasing the evaporative losses due to greater partitioning of incoming precipitation into interception (E_i, Kergoat, 1998), although this might not be the case in forests with vertically-angled leaves where increased *L* is unlikely to contribute to greater throughfall (Crockford & Richardson, 2000). Additionally, increased foliage shading decreases the amount of radiation reaching the ground surface, thus decreasing understorey transpiration and soil evaporation (Crockford & Richardson, 2000, Raz-Yaseef *et al.*, 2010). Ultimately, the contribution of these later components will be strongly determined by the amount and characteristics of the precipitation events and the dynamics of atmospheric evaporative demand.

Predictions of the impact of eC_a on forest hydrology are largely derived from leaf-level studies (Field *et al.*, 1995, Gimeno *et al*., 2016), models (Betts *et al.*, 2007) and retrospective analyses (Yang *et al.*, 2016b), with additional insights from Free-Air CO_2 Enrichment (FACE) experiments conducted in forests (Donohue *et al.*, 2017). Some of these FACE studies found partial reductions in g_s (Ellsworth, 1999, Gimeno *et al.*, 2016, Gunderson *et al.*, 2002, Keel *et al.*, 2007) and reduced canopy-transpiration (Cech *et al.*, 2003, Wullschleger & Norby, 2001), while others did not find a reduction in either leaf- or canopy-level transpiration (Uddling *et al.*, 2009, Ward *et al.*, 2013). In addition, leaf-level water savings were often offset by increased L (Bobich *et al.*, 2010, Schäfer *et al.*, 2002, Tor-ngern *et al.*, 2015, Warren *et al.*, 2011). All of these studies focused mainly on the effect of eC_a on canopy transpiration (E_{tree}), while other components of evapotranspiration (E_t) were rarely measured (Cheng *et al.*, 2017, but see Schäfer *et al.*, 2002). Furthermore, these studies are primarily restricted to energy-limited or moderately water-limited young trees or forest plantations (Bobich *et al.*, 2010, Ellsworth, 1999, Godbold *et al.*, 2014). In water-limited woodlands, we are less likely to observe a change in R or D_g under eC_a, as potential increases in soil moisture could be lost via ground evaporation and understorey transpiration (Ferretti *et al.*, 2003, Nolan *et al.*, 2014, Nowak *et al.*, 2004), although this could be partially offset by reduced g_s under eC_a in the understorey (Morgan *et al.*, 2004). Notwithstanding previous work in tree plantations (Schäfer *et al.*, 2002, Uddling *et al.*, 2009, Wullschleger & Norby, 2001), we still lack an experimental test of the effects of eC_a on hydrological partitioning, particularly in mature woodlands experiencing potential water deficits throughout the year. To validate dynamic vegetation models for predicting vegetation-climatic feedbacks, large-scale observations simultaneously addressing the impact of eC_a on all E_t components (not just E_{tree}), R and φS are desperately needed (Fisher *et al.*, 2017, Porporato *et al.*, 2004).

In our study, a mature and water-limited *Eucalyptus* woodland was exposed to a C_a 150 µmol mol^{-1} above ambient, using Free-Air CO_2 Enrichment (the óEucFACEô experiment). Here, we address the effects of eC_a on precipitation partitioning among components of the hydrological balance (E_t, R, D_g and φS) over the first two years of the EucFACE experiment. Duursma *et al.* (2016) demonstrated that L did not respond to eC_a in this woodland, so we hypothesized (*i*) that partial stomatal closure at the leaf-level (Gimeno *et al.*, 2016) would lead to a decrease in E_{tree} under eC_a; however, since g_s did not decrease under eC_a in the understorey (Pathare *et al.*, 2017) we expected (*ii*) that excess water ósavedô by the canopy would be lost via increased soil evaporation together with understorey transpiration (E_{floor}), (*iii*) thus resulting into no net increase in φS, R or D_g. The lack of structural changes induced by eC_a in this timeframe (Duursma *et al.*, 2016), means that we have the advantage that we can carefully examine the partitioning of eC_a effects on water balance components without being confounded by stand structure effects.

Materials and Methods

Study site and experimental design

EucFACE is located on an ancient alluvial þoodplain, 3.6 km from the Hawkesbury River, in western Sydney (NSW, Australia, 33°37'S, 150°44'E, 23 m a.s.l.), in a 270 ha patch of native Cumberland Plain woodland (Fig. S1). The site is flat (maximum slope: 0.004°), with the lowest land-surface elevations found near ring 5 (Fig. S1). The site is characterized by a humid temperate-subtropical transitional climate with a mean annual temperature of 17ºC, with January being the hottest (mean daily maximum 30ºC) and July the coldest (mean daily minimum 3.6ºC), and a mean annual precipitation (P) of 730 ± 30 mm y^{-1}, with February being the wettest month (123 ± 16 mm month^{-1}) and July the driest (29 ± 5 mm month^{-1}, mean ± se, 1992-2014, Bureau of Meteorology, station 067105, 5 km away). Satellite-estimated actual E_t is 739 ± 34 mm y^{-1} (1981-2012, Zhang *et al.*, 2016), which means that the site is water-limited.

The upper soil (up to 30-50 cm) is a loamy sand (> 75% sand), slightly-acidic (pH = 4.5) and with low-organic C (< 1%) and overall low phosphorus (Ellsworth *et al.*, 2017). At 30-70 cm depth, there is a layer of higher clay content (15-35% clay), below which the soil is a sandy loam or sandy clay loam. Between 300-350 and 450 cm depth, the soil is clay (> 40% clay). Groundwater is present at ~12 m below the surface (Fig. S2).

Tree density ranges from 600-1000 trees ha^{-1} (basal area, BA = 27.6 ± 2.7 m^2 ha^{-1}, n = 6 plots), L is Ò2 m^2 m^{-2} (Duursma *et al.*, 2016), the canopy height is 18-23 m tall and mean tree diameter at 1.3 m (DBH) is 18.8 ± 0.6 cm. The main canopy forming tree is *Eucalyptus tereticornis* Sm with an understory mainly composed of grasses, with low densities of forbs and occasional shrubs (Pathare *et al.*, 2017).

At EucFACE, there are six 25-m diameter plots (hereafter óringsô). Each ring comprises a cylindrical frame of 28 m-high vertical pipes extending above the canopy (treetops ranging 18-23 m). Vegetation within rings 1, 4 and 5 (Fig. S1) was exposed to a C_a 150 µmol mol^{-1} above ambient, whereas the other three rings received ambient C_a (see Gimeno *et al.*, 2016 for further details). In contrast to previous FACE experiments, here C_a was ramped-up gradually to minimize potential transient effects. Here, the C_a was increased at a rate of ~30 µmol mol^{-1} per month over a ~6 month period until C_a reached 150 µmol mol^{-1} above ambient in the eC_a rings on the 5 February 2013 (see Drake *et al.*, 2016 for a detailed description of the ramp-up).

Meteorological and soil moisture measurements

On top of a central tower (23.5 m) in each ring, an array of sensors measured air temperature and relative humidity (HUMICAP ® HMP 155, Vaisala, Vantaa, Finland), net radiation (R_n, CNR2 Kipp & Zonen, Delf, The Netherlands), photosynthetically active radiation (PAR, LI-190, LI-COR, Inc., Lincoln, NE, USA) and wind speed (Wincap Ultrasonic WMT700 Vaisala, only on the three eC_a rings, Fig. S1). These variables were measured every second and one- (wind) or ten-minute (all other variables) averages were recorded on data loggers (CR3000, Campbell Scientific Australia, Townsville, Australia). The average of the six (three for wind) rings was used to characterize the meteorological conditions on site. Daily Penman potential evapotranspiration (E_p) was calculated as (Donohue *et al.*, 2010):

(Eq. 1)

$$E_p = \frac{\Delta}{\Delta + \gamma} R_n + \frac{\gamma}{\Delta + \gamma} \frac{6430(1 + 0.536u)D}{\lambda}$$

where γ is the psychrometric constant (65.3 Pa K^{-1}), daily R_n integral is in mm day^{-1}, D is mean daily water vapour pressure deficit (in Pa), u is mean daily wind speed (in m s^{-1}), λ is the latent heat of vaporisation of water (2.45 MJ kg^{-1}) and Δ is the rate of change of saturated water vapour with temperature (Pa K^{-1}).

Soil volumetric water content (θ_v) was monitored in each ring at eight locations with frequency-domain reflectometers installed at 30 cm depth (TDRs, CS650 Soil Water Content Reflectometer, Campbell Scientific). Soil temperature (T_{soil}) was measured at two locations in each ring with temperature probes at 5 cm depth (TH3-s, UMS GmbH, Frankfurt, Germany). θ_v and T_{soil} were measured every second and 15-minute averages were logged on CR3000s.

Canopy leaf area measurements

A detailed description of the methods for L (in m^2 m^{-2}) quantification is found in Duursma *et al.* (2016). Briefly, L was estimated from diffuse canopy transmittance (τ_d) calculated from the ratio of above- and below-canopy PAR measured in each ring with one and three sensors (LI-190), at 23.5 and 1.5 m height, respectively. For these calculations we used only PAR measurements under highly diffuse conditions (diffuse fraction [F_{diff}] > 0.98). We measured F_{diff} with a BF5 Sunshine sensor (Delta-T Instruments, Cambridge, UK) installed on a tower extending 5 m above the canopy at a nearby site (within 2 km). We then calibrated *L* estimates from Ǘd against cumulative litter production over 4-months (Duursma *et al.*, 2016).

The water balance components

Mass balance provides a framework for assessing the impact of eC_a on the partitioning of precipitation (*P*). The mass balance for water can be expressed as:

(Eq. 2)

$$P = R + D_g + \Delta S + E_t$$

where *R* is surface runoff, D_g is drainage, φ*S* is the change in root-zone soil water storage and E_t is evapotranspiration. All variables measured in mm day^{-1}. In this study, we assessed the effect of eC_a on E_t and φ*S*, while we did not expect a significant effect on *R* or D_g. Therefore, φ*S*, E_t and all of its components were quantified at the ring-level (except for stem-flow, see below) and *R* and D_g at the site-level. Eq. 2 was implemented for 30 months starting on June 2012, including the pre-treatment and ramp-up periods

1. *Precipitation*

We defined a *P* event as a continuous series of hours with $P > 0$ mm h^{-1} interrupted for one hour or less with $P = 0$ mm h^{-1}. Site *P* was the average of three automated tipping bucket rain gauges (TB4, Hydrological Services Pty Ltd, Liverpool, NSW, Australia) located at the top of the central tower in rings 1, 4 and 3 (Fig. S1). *P* from each bucket was logged every 15 minutes onto CR3000 data loggers.

2. *Surface runoff*

Surface runoff (R) was calculated as the excess of P minus E_p when the upper soil was saturated and precipitation intensity either exceeded soil infiltration capacity (17 mm h^{-1} for sandy soils, Campbell & Norman, 1998) or cumulative precipitation (P_{cum}) for each event minus E_p exceeded maximum soil storage capacity. In our site, with a sandy soil with $\theta_v = 3\%$ at permanent wilting point and $\theta_v = 30\%$ at saturation and an effective depth of 400 mm, the maximum soil storage capacity was calculated as: 400 × (30-3)/100 = 108 mm. This approach should be valid for our flat study site with a stratified (or duplex) soil texture with a defined shallow layer of relatively impermeable clay at ~400 mm.

3. *Drainage and soil water*

The D_g from Eq. 2 represents the amount of water that drained below the assumed root-zone and was not accessible for transpiration. To determine whether the vegetation in our study site was accessing groundwater, we monitored changes of the water table level on-site and analysed the isotopic composition of xylem water and potential water sources (Supplementary methods). Neither the dynamics of the water table depth (seasonal or intra-day), nor the isotopic composition of the tree xylem water suggested that the vegetation at our site used groundwater (Fig. S2 and S3).

We assumed that D_g would be water lost from the deep soil layer and calculated D_g as the inverse of the change in soil water storage from 3 to 4.5 m depth. This approach was justified for our site where the soil has a marked multilayered texture: the upper sandy soil (from 0 to 0.3-0.5 m) is where the majority of roots are located (Piñeiro et al., unpublished data). Below this depth (up to 3 m), the soil is a sandy clay loam (up to 3 m depth) where only a few live roots are present and below 3 m, a clay horizon starts and continues beyond 4.5 m depth. Our observations for root distribution across the depth profile are consistent with the results of Macinnis-Ng *et al.* (2010) from a nearby (within 7 km) site where ~90% of the tree roots were found in the upper soil (0.7 m) with only occasional roots present in the deeper (up to 1.5 m) clay horizon. We assumed that changes in soil moisture below 3 m are unlikely affected by direct vegetation water uptake or hydraulic lift. Thus, we calculated D_g as water lost below 3 m for a given time interval (t_1-t_2) according to:

(Eq. 3)

$$D_{g,t_1-t_2} = -\sum_{i=3}^{z_{max}} \left(\theta_{i,t_2} - \theta_{i,t_1}\right)\left(z_i - z_{i-1}\right)$$

where $\theta_{i,t}$ is the soil water content at depth z_i and z_{max} is 4.5 m (Duursma *et al.*, 2011). There were no differences in deep soil water storage between ambient and eC_a rings over time (t = -0.94, p = 0.35), so D_g was calculated at the site level from averaged deep soil water storage from all rings.

Soil volumetric water content (θ_v) across the soil profile (25-450 cm) was monitored every 15-20 days at two locations in each ring with a neutron probe (NMM, 503DR Hydroprobe ®, Instroteck, NC, USA). We measured θ_v in 25 cm intervals from 25 to 150 cm depth and in 50 cm intervals from 150 to 450 cm depth (see Supplementary Methods).

4. *Change in soil water storage*

We calculated the change in soil water storage (ΔS) for a soil column to 3 m depth. Since we expected to observe an effect of eC_a on ΔS, we calculated ΔS for each ring over a given time (t) interval (t_1-t_2) as:

(Eq. 4)

$$\Delta S_{t_1-t_2} = \sum_{i=0}^{z_{max}} \left(\theta_{i,t_2} - \theta_{i,t_1}\right)\left(z_i - z_{i-1}\right)$$

where θ_i is the soil water content at depth z_i and z_{max} is 3 m (Duursma *et al.*, 2011). Here, θ_i is the mean of two measurements at the same depth from two locations within each ring.

5. *Evapotranspiration*

Total ecosystem evapotranspiration (E_t) consists of:

(Eq. 5)

$$E_t = E_i + E_{tree} + E_{floor}$$

where E_i is the canopy interception loss, E_{tree} is overstorey canopy transpiration and E_{floor} is soil evaporation and understorey transpiration.

a. Interception

Canopy interception loss (E_i) was calculated as:

(Eq. 6)

$$E_i = P - (T_f + S_f)$$

where T_f is throughfall and S_f is stemflow. Throughfall (T_f) was measured under the canopy with one custom-built fixed trough in each ring. Each trough consisted of an 8 × 0.25 m gutter set with a maximum inclination of 1°. In each ring, T_f was calculated taking into account the projected area of each gutter. The troughs drained into a large volume tipping bucket flow gauge (TB1L, Hydrological Services Pty Ltd). Total T_f was logged every 15-minutes onto CR3000 data loggers. One additional trough was located in an open space (Fig. S1) to act as a control and we found that this trough underestimated P by 4.4 ± 0.6% ($R^2 = 0.98$, $p < 0.001$). We assumed that the throughs in the rings underestimated T_f to a similar extent to the control through and corrected accordingly to calculate E_i.

Stem flow (S_f) was measured in ten trees across EucFACE, adjacent to the study rings, (DBH: 24.6 ± 2.4 cm, range: 14-38 cm). Stem flow collectors were custom-built and consisted of a collar, constructed from a half-split 25 mm diameter vinyl pipe glued with silicone around the trunk. Collectors channelled S_f into automated tipping buckets (TB4) and total S_f was recorded every 15 minutes onto a CR3000. We used this dataset to model the amount of S_f in each ring. We fitted a linear mixed model to S_f volume collected in each precipitation event as a function of tree basal area, P event size and duration (Crockford & Richardson, 2000), including event as a random factor (Table S1). The obtained coefficients for each fixed factor (tree basal area, P_{cum} and duration) were used to predict S_f of each tree inside each ring, during each precipitation event.

b. Overstorey canopy transpiration

Whole tree overstorey canopy transpiration (E_{tree}) was computed from measurements of tree sapflow velocity (v_s, Oren *et al.*, 1998). We measured v_s every ten minutes using the heat pulse compensation technique (Marshall, 1958) with equipment manufactured by Edwards Industries (Havelock North, New Zealand) and connected to a CR3000 data loggers. Each sensor consisted of two temperature probes, constructed of sealed Teflon ® 1.8 mm diameter tubing, with each probe containing a negative temperature coefficient thermistor. The temperature sensors were placed 10 mm (downstream) and 5 mm (upstream) from a 1.8 mm diameter stainless steel heater probe. The holes for the temperature and heater probe were drilled with a drill guide to ensure accurate positioning of the probes and parallel alignment. Distances between implanted probes and bark depth were recorded at the time of installation. Measured heat pulse velocity was corrected for the appropriate wound size. The wound width was measured from cut sections of sapwood where ódummyô probes were inserted for 30 days from five trees adjacent to the study plots. Wound size (2.7 ± 0.2 mm) was measured under the light microscope (×40 magnification). v_s was calculated from heat pulse velocity given the fractions of wood and liquid in the sapwood (Swanson & Whitfield, 1981).

In winter 2012, four dominant or co-dominant trees with positive growth rates for the previous year were selected for monitoring of v_s, in each ring. Two sets of thermocouples and heater element were installed in each tree at 1.3 m height on two randomly selected azimuths. At each tree location, the two thermocouples were positioned at the specific depth below the cambium at which v_s was maximised along the sapwood profile (i.e. both probes in each tree were set at the same depth to get an estimate of within tree radial v_s variability). This depth was determined empirically for each tree as follows: within each tree, one probe was set at

10 mm below the cambium (fixed) and the second probe (mobile) at 25 mm below the cambium. Then, on a cloudless spring day in September 2012, the mobile probe was incrementally pulled out from 25 to 0 mm below the cambium at 5 mm intervals every 90 minutes (Wullschleger & Norby, 2001). In sensors that were not manipulated, v_s remained relatively constant. With these observations, we determined the depth below the cambium at which v_s was maximal by comparing v_s between the fixed and the mobile probe.

Sapwood area (A_s) and fractions of wood and liquid within the sapwood matrix were calculated from cores extracted from 35 trees adjacent to the study rings. Cores were collected from trees reflecting the size distribution of trees within the rings (DBH: 31.3 ± 2.2 cm). Wood cores were 5 mm in diameter and were extracted using a standard Pressler increment borer (Haglöf Västernorrland, Sweden). Sapwood depth was measured with a digital calliper after staining wood cores with methyl-orange that provided visual differentiation of the sapwood from the heartwood (Pfautsch *et al.*, 2012). We calculated the correlation coefficients between basal area and A_s measured in these trees to predict A_s per unit of ground area from basal area inside each ring.

Mean tree v_s was calculated from the average of the two sets of thermocouples and heater element installed on each tree. We calculated mean hourly v_s for each ring ($\bar{v}_s$) from the four (three in rings 2 and 6) measured trees. Hourly E_{tree} for each ring was calculated as:
(Eq. 7)

$$E_{tree} = A_s \bar{v}_s$$

where A_s is the sapwood area per unit of ground area of each ring. Daily and seasonal water-use per unit ground area for each ring were calculated by integrating E_{tree} over time.

c. Soil evaporation and understorey transpiration

Soil evaporation together with understorey transpiration (E_{floor}) was estimated from the change in soil moisture over 5 cm depth measured at two locations in each ring with two theta probes (ThetaProbe ML2x, Delta-T). Changes in soil moisture at this depth are likely to reflect E_{floor} because: (*i*) most understorey vegetation roots are found between 0 and 5 cm depth (Piñeiro et al. unpublished data); and (*ii*) changes in soil moisture at this depth are likely to capture water losses due to soil evaporation, given the soil's sandy texture (Campbell & Norman, 1998). Hourly E_{floor} was calculated as:

(Eq. 8)

$$E_{\text{floor},t_2-t_1} = z\,\Delta\theta_{t_2-t_1}$$

where z is the depth of the theta probes (5 cm) and $\Delta\theta_{v,t_2-t_1}$ is the difference in θ_v between consecutive hourly averages (t_1-t_2). A decrease in θ_v from 0 to 5 cm results from evapotranspiration, but also from water infiltration (Schreiner-McGraw *et al.*, 2016); thus, to avoid overestimation of E_{floor}, we only calculated E_{floor} for days with $P = 0$ mm d^{-1} and preceded by a day with $P < 2$ mm d^{-1} (454 of 730 days passed these criteria). We validated our approach with E_{floor} measurements made at one location adjacent to ring 1 (Fig. S1). An automated long-term clear chamber (LI-8100-104C, LI-COR,) coupled to an IRGA (LI-8100A, LI-COR) measured E_{floor} every 30 min on a permanently installed PVC collar. The automated chamber was deployed from winter 2013 to spring 2014 and rendered 222 days of measurements without errors (Fig. S4). We found that E_{floor} measured with the clear chamber followed an exponential correlation with site E_p (Fig. S4). Also, daily E_{floor} estimated from $\Delta\theta$ was significantly correlated with daily E_{floor} measured with the clear chamber ($p < 0.05$, Fig. S4). For those dates with $P > 0$ mm d^{-1} and/or preceded by a day with $P \geq 2$ mm d^{-1} (276 days), E_{floor} was estimated from site E_p, from the exponential correlation of E_{floor} and E_p from the clear chamber measurements (Fig. S4).

Statistical analyses

We tested for significant differences ($p < 0.05$) between C_a levels over time on E_{tree}, E_{floor} and soil water storage by fitting general additive mixed models (GAMMs). For this purpose, we considered the ring as our experimental unit and assessed for random ring-to-ring variability within each C_a level (Wood, 2006). We used the *mgcv* package in R version 3.2.2 (R Development Core Team, 2014). In all fitted GAMMs, we used a cubic regression spline. For the smoothed term in the model, we used up to 5-20 degrees of freedom, which resulted in biologically realistic smoothed dynamics. Additionally, to quantify soil water dynamics under ambient and eC_a, irrespective of horizontal and vertical heterogeneity in soil texture, we estimated the numerical derivative of soil water storage (dS/dt) and its confidence interval (Duursma *et al.*, 2016) as estimated from the GAMM fitted to dS/dt for ambient and eC_a, for the whole vertical profile (0-4.5 m) and for specific depths.

To assess the effect of eC_a on the relationships between climatic (D, T_{soil} and PAR) and other environmental drivers (θ_v and L) and transpiration components (E_i, E_{tree}, E_{floor}), we used either GAMMs or linear mixed models (LMM). We used a LMM to assess the effects of eC_a on the relationships of E_i with L; precipitation event duration and size; with ring and precipitation event as random factors. We used GAMMs to test for the effect of eC_a on the climatic forcing of E_{tree} and E_{floor}, with ring and date as random factors. For E_{tree}, we included D, u and PAR as predictors and L as a covariate (Duursma *et al.*, 2014). To further asses the eC_a effect on the climatic forcing of E_{tree} we performed an additional GAMM with day-length normalised D (D_z, Tor-ngren *et al.*, 2015). For E_{floor} (computed only from $\varphi\theta$ measured inside the rings), we included understorey D and PAR, T_{soil} and θ_v (Raz-Yaseef *et al.*, 2012).

We estimated our ability to close the water balance by calculating P minus ($R + D_g + \varphi S + E_t$) from Eq. 2. We computed the overall water balance for the study site, with site P, R, D_g and average ($n = 6$ rings) φS and E_t. We calculated the terms of the water balance for each season (summer, DJF; autumn, MAM; winter, JJA; and spring, SON). We considered that we had closed the water balance when the sum of the water balance components (Eq. 2) was at least 75% of precipitation for that period, i.e. $|(P - R + D_g + \varphi S + E_t)/P| < 0.25$ (Schreiner-McGraw *et al.*, 2016).

Results

Meteorological parameters and precipitation

All the data and analyses presented in this manuscript are published here for the first time, except for the raw climatic data (temperature, precipitation and air relative humidity, Gimeno *et al.,* 2016) and the leaf area index (L, Duursma *et al.,* 2016). Prior to the start of the eC_a treatment, the EucFACE site experienced a very wet summer and early autumn (P_{cum} December 2011-April 2012: 647 mm, or 2/3rds of long-term annual average), followed by an average autumn and winter. During the eC_a ramp-up, the site experienced a wet and warm spring and summer, and a heat wave when we recorded the highest D on site for the study period (7.9 kPa, Fig. 1). In late January 2013, the site received P_{cum} = 191 mm in 7 days (Fig. 2) that led to temporary standing water on site for 48 h. The first year of full eC_a treatment (commencing on February 2013) was characterized by a warm and dry winter, followed by an unusually hot and dry early spring that boosted daily D and E_p close to typical midsummer values (Fig. 1). This was followed by a rainy spring (P_{cum} = 218 mm in November 2013, Fig. 2) that preceded a drier than usual summer (P_{cum} = 87 mm in February 2014) and finally an average autumn and winter in 2014 (Fig. 1, Table 1).

Surface runoff, drainage and groundwater depth

Over the study period, P_{cum} exceeded maximum soil water storage capacity (108 mm) during one precipitation event (27 January 2013; Fig. 2) with an excess of 39 mm over 24 h. During this period E_p was 8 mm, so R was estimated as 31 mm (Table 1). Furthermore, the site experienced one event (15 November 2013) that should have exceeded soil infiltration capacity, but the soil was not saturated and standing water was absorbed before any R was generated.

From July 2013 to October 2014, mean groundwater depth was 12.8 m and ranged from 12.64 to 12.96 m. The variability in the groundwater depth did not show any daily or seasonal patterns (Fig. S2). The isotopic signature of xylem water under dry and wet conditions did not match the signature of groundwater (Fig. S3). These analyses, together with the absence of live roots below 1 m depth observed during the augering of 15 holes of 4.5 m depth each, suggests that the EucFACE deep-rooted vegetation (trees) did not access groundwater. Henceforth, we argue that observed changes in the groundwater depth were likely associated with regional groundwater ï surface water interactions governed by the water-level in the Hawkesbury River. Our approach to calculate D_g (Eq. 3) should be valid for the temporal (2 years) and spatial (~1 ha of instrumented study area) scale of this study.

The contribution of D_g to the water balance varied from 20% (spring 2012) to 2% in summer 2013 (Table 1), although it should be noted that seasonal D_g and P could be temporally uncoupled. Coupling depends on the P dynamics and the level of antecedent saturation in the soil column. At our site, D_g might be lagged with respect to seasonal P when the upper soil column (0-3 m, sand and sandy clay loam) was saturated with water, but not the deep soil (below 3 m, clay). This would have led to an initial increase in deep soil water storage that would have later drained below the root-zone. This was the case in autumn 2013 when D_g according to our calculation was negative (i.e. apparent reduction in the amount of water below the rooting zone). With the exception of this latter season, our approach showed that over the study period, there was an excess of water draining beyond the root zone.

Effect of elevated CO_2 on soil water storage (S)

Initial measurements of S (June 2012) were the maximum over the study period. S_{max} varied among rings due to differences in soil texture (ring 6 with the highest clay content had the highest S_{max}: 828 mm) and micro-topography (S_{max} in ring 5 with the lowest elevation was 758 mm, while in ring 1: 657 mm). We found that S decreased continuously in all rings during 2012, until early 2013, when large precipitation events increased S close to S_{max} (Figs. 2 and 3a). In 2013, S also decreased until another series of rain events in November, when S increased, but did not reach S_{max} (Fig. 3a). During the first half of 2014, S decreased until a series of precipitation events in the middle of the year (August) interrupted this trend (Fig. 3a), yet S did not reach S_{max}. The complete overlapping of the 95% CI of the fitted GAMM to S over time between C_a levels indicated that there were no significant differences in S between C_a levels (Fig. 3a). Similarly, we found that S integrated over 0.25 or 0.5 m depth intervals did not differ between C_a (Fig. S5).

We found that S decreased significantly for most of the study period, ($dS/dt < 0$, $p < 0.05$), particularly during the autumn-winter (Fig. 3b). During wet periods, S increased, but dS/dt was significantly positive only in summer 2013 and spring 2014. The 95% CI of the fitted GAMM for ambient and eC_a overlapped over the entire period, indicating that there were no significant differences in dS/dt (Fig. 3b). We found similar results for dS/dt calculated for specific depths up to 2 m (Fig. S6). Below 2 m depth, in 2012 (pre-treatment and ramp-up), dS/dt in eC_a was positive or zero when our measurements commenced and then it declined progressively to stable negative values, non-significantly different from those in ambient C_a. This result was strongly driven by the contrasting trends observed in two of the study rings that happened to be randomly assigned to different C_a levels and it is not likely to have been generated by the eC_a treatment *per se*. Instead, this resulted from the preceding heavy rainfall that most likely led to lateral water redistribution towards ring 5, which has the lowest elevation and which happened to be randomly assigned to the eC_a treatment. Additionally, this could have also resulted from a greater rate of soil water decline observed in one of the ambient C_a rings (ring 6), which was not mimicked by the other two ambient rings (2 and 3), but yet affected the overall mean of the ambient C_a treatment. We suggest that vertical heterogeneity in the soil texture structure was responsible for differences among ambient C_a rings.

Stem flow, throughflow and interception under elevated CO_2

We found that S_f, measured adjacent to the EucFACE rings, was significantly correlated ($p < 0.001$) to tree basal area, and the quantity and duration of P events (Table S1). The estimated contribution of S_f within each ring was less than 2% of precipitation.

E_i did not differ between C_a levels (Table 2). The best model for E_i included L, quantity and duration of the P event, but it did not include C_a, or its interactions (Table 2). Since L did not respond to eC_a, indirect eC_a effects on E_i were discarded. Across the seasons, the contribution of E_i to E_t was not negligible (Fig. 4) and ranged from 5% (in winter 2013) to 24% (summer 2013). The main driver of E_i was P_{cum} (Table 2) so differences in the relative contribution of E_i to E_t between years and within season were due to differences in P (Fig. 4 and Table S2).

Canopy transpiration and understorey evapotranspiration under elevated CO_2

A leaf flushing event occurred shortly after the start of the implementation of the full eC_a treatment, thus the potential direct effect of eC_a on leaf-level transpiration would have been realized since the beginning of the experimental treatment. Over the study period, neither E_{tree}, nor E_{floor} differed between C_a levels, as evidenced by the consistent overlap of the 95% GAMM confidence intervals (Fig. 5, 6, S7 and S8). E_{tree} constituted the largest proportion of seasonal E_t, followed by E_{floor}, in all seasons (Fig. 4). The mean contributions of E_{tree} and E_{floor} to E_t were 63% and 20%, respectively, and ranged from 72% (winter 2013) to 58% (summer 2013) for E_{tree} and from 23% (spring 2013) to 15% (winter 2014) for E_{floor}. Daily E_{tree} showed the typical three phase response to D_z variation, initially rising with increasing D_z until it reached a plateau and then decreasing, with no significant differences between C_a levels (Fig. 6). The GAMM also showed that E_{tree} was strongly driven by total daily PAR, again with no significant differences between C_a levels (Fig. S7). E_{floor} was strongly controlled by θ_v followed by T_{soil} and understorey D with no significant differences between C_a levels (Fig. S8).

The overall water balance

We quantified the water balance components for our site and according to our criteria, $|(P - R - D_g - \varphi S - E_t)/P| < 0.25$, we achieved good closure in summer and spring 2013 and in winter 2014. Also, we were able to account for 44% of P in winter 2013 (Table 3). We were unable to close the water balance in spring 2012, autumn 2013 and summer 2014; three seasons preceded by large precipitation events (Fig. 2), when soil water storage increased by more than 100 mm (Table 1).

Discussion

Our study constitutes the most comprehensive quantification of the hydrological balance of a tree-dominated FACE experiment (Leuzinger & Körner, 2010, Schäfer *et al.*, 2002). Previous forest FACE studies found reduced tree water-use (Warren *et al.*, 2011) but neglected the eC_a effect on understorey evapotranspiration (except from Schäfer *et al.*, 2002) or on the partitioning to φ*S*, D_g and *R*. Furthermore, none of these were conducted in water-limited sites and while some climatic land-surface models predict an increase in φ*S* and eventually in *R* and D_g (Betts *et al.*, 2007, Gedney *et al.*, 2006); this prediction does not appear to hold for water-limited regions (Ukkola *et al.*, 2016). Furthermore, all these predictions are based on retrospective analyses and thus are limited to present-day C_a and cannot account for projected C_a increases for most of the 21st century. For water-limited regions, process-based theoretical models predict that increased *L* offsets reduced leaf-level transpiration under eC_a (Donohue *et al.*, 2017, Macinnis-Ng *et al.*, 2011). Here, for our water-limited woodland, we had hypothesised that reduced E_{tree} under eC_a, would not be offset by increased *L* (Duursma *et al.*, 2016) and since the site is water-limited, any excess water resulting from reduced E_{tree} would be quickly lost via E_{floor}, meaning no net increase in φ*S*. We found no changes in E_{tree}, E_{floor} or φ*S*, thus eC_a did not reduce stand water-use in this mature water-limited woodland.

Canopy transpiration under ambient and elevated CO_2

Contrary to our expectations, we did not find a reduction in E_{tree} under eC_a, neither in daily mean nor maximum v_s. Some previous forest FACE studies had found non-significant reductions in E_{tree} under eC_a (Bobich *et al.*, 2010, Ward *et al.*, 2013); but in these studies, reductions in leaf-level transpiration were offset by increased *L*, which we did not observe (Duursma *et al.*, 2016). In our case, g_s of the canopy-dominant tree (*E. tereticornis*) temporary decreased by 20%, but this reduction was transient and became non-significant when water availability became most limiting and *D* peaked (Gimeno *et al.*, 2016). Furthermore, any given decrease in g_s is usually translated into a weaker transpiration response because there are additional sources of variability affecting the upscaling from leaf-to canopy-level processes such as micrometeorology, canopy patchiness and/or vertical variations in leaf anatomy, even in well-coupled canopies, such as ours (Jarvis & McNaughton, 1986). Hence it is not surprising that the partial reduction observed in g_s from discrete campaigns restricted to the upper part of dominant trees did not scale to the canopy level. Additionally, our observations from this native woodland are inherently affected by the natural variability. For example, the mean coefficient of variation for mean daily v_s within rings (i.e. among trees) was 38%, whereas within C_a levels (i.e. among rings) it was 24%, despite selection of the most representative and comparable trees that contributed up to 50% of the total basal area within each ring. Given that maximum measured reduction in g_s was 20% (Gimeno *et al.*, 2016); we cannot discard that potential transient reductions in canopy transpiration could have been obscured by the natural variability among trees for this two-year study (Paschalis *et al.*, 2017).

Besides the expected direct effect of eC_a on E_{tree}, we also expected indirect effects, beyond changes in L that did not occur (Duursma *et al.*, 2016). Elevated C_a could have also indirectly affected E_{tree} by modifying climatic forcing of transpiration; for example, the slope of the relationship between D and transpiration can decrease under eC_a (Duursma *et al.*, 2014, Wullschleger & Norby, 2001). In our study, there were no significant differences between C_a levels in the response of E_{tree} to D, including a much larger D (up to 7.9 kPa) than experienced previously at another forested FACE experiment (Tor-ngern *et al.*, 2015). This result is consistent with the lack of a significant effect of eC_a on the combined sensitivity of stomata to C_a and D in eucalypts (Gimeno *et al.*, 2016, Kelly *et al.*, 2016). Taken together, these results suggest that eC_a is unlikely to alleviate increasing atmospheric drought stress in a climate change scenario with warmer temperatures and higher D (Nelson *et al.*, 2004), at least in this mature eucalypt woodland.

Understorey evapotranspiration and canopy interception under elevated CO_2

We had hypothesised that excess water resulting from reduced E_{tree} under eC_a would be lost via enhanced E_{floor}, but here, E_{tree} did not decrease under eC_a and there was no increase in E_{floor}. Consistently, soil water storage (S) did not differ between ambient and eC_a plots at any depth and neither did φS over the study period, which vertically extends similar results for the upper soil (0-30 cm) on the same site (Drake *et al.*, 2016, Pathare *et al.*, 2017). Previous studies had reported that soil moisture was not conserved in eC_a in water-limited regions (Nowak *et al.*, 2004) and without increased water availability; it is not surprising that there was no change in E_{floor}. We did not find an indirect effect on E_{floor} either, as the response of E_{floor} to T_{soil} and θ_v was unaffected by eC_a. With our approach, we cannot separate the contributions of understorey transpiration and soil evaporation to E_{floor}, which in this type of woodland are both likely to constitute an important fraction of ecosystem water-use (Ferretti *et al.*, 2003, Nolan *et al.*, 2014). In our study, the evaporative component could not have been affected by eC_a because soil water did not increase (Drake *et al.*, 2016) and the amount of incident radiation in the understorey did not decrease, as L was unaffected (Duursma *et al.*, 2016). In contrast, we could have still expected that transpiration by the understorey responded to eC_a, in addition to indirect environmental effects (via changes in soil moisture or incident radiation). Nevertheless, three years of measurements on the dominant understorey grasses on-site revealed that under eC_a neither g_s decreased, nor did herbaceous biomass increase (Collins *et al.*, 2018, Pathare *et al.*, 2017).

We quantified the contribution of E_i to E_t and whether this component changed under eC_a. In agreement with previous studies (Crockford & Richardson, 2000, Gash, 1979, Soubie *et al.*, 2016), quantity and duration of the P events were the main drivers of E_i, T_f and S_f. More abundant and longer events resulted into larger E_i, but contrary to expectations, we found a negative effect of L on E_i. The prediction that E_i increases with L is based on observations from densely packed canopies with horizontally angled leaves (Kergoat, 1998). However, in most *Eucalypt* woodlands, including ours, leaves are angled vertically or near-vertically; hence, P falling on the vegetation mostly contributes to T_f instead of E_i (Crockford & Richardson, 2000). Nevertheless, given that neither L (Duursma *et al.*, 2016) nor tree radial growth rate increased under eC_a (Ellsworth *et al.*, 2017), we are unlikely to observe any change in the partitioning of P into T_f, S_f and E_i under eC_a, in mature *Eucalypt* woodlands. Even under a scenario where L and/or growth responded to eC_a, we would still predict that E_i would not change because the contribution of S_f is negligible (and thus so would be potential increases in S_f due to radial growth increments) and greater L would not increase E_i with these leaf angles. This later result is relevant for improving our ability to estimate ecosystem water-use and to predict vegetation-atmospheric coupling under future atmospheric conditions. Currently, most process-based models assume that E_i increases with eC_a (De Kauwe *et al.*, 2013, Zhang *et al.*, 2016), but our results suggest otherwise for this type of woodland, over the study period.

Lack of effective water-savings under elevated CO_2

Over the study period, potential evapotranspiration (E_p) exceeded precipitation (P) in all seasons and total E_t was always less than E_p, which indicates that our site was water-limited during the study period, at this time-step. We found that despite being water-limited, seasonal E_t was often less than P, which allowed some P to be partitioned to ϕS, R and D_g. Here, we followed a conservative approach to calculate D_g from deep soil water dynamics assuming an effective rooting depth of 3 m. With this approach, we are likely overestimating the decrease (or underestimating the increase) in ϕS and thus we are underestimating the amount partitioned to D_g. For those seasons where we calculated a decrease in ϕS, our estimate of E_t was not similar to ϕS plus P, minus R and D_g. Our estimates of E_{tree} and E_{floor} are comparable to observations from similar (Nolan *et al.*, 2014) and nearby forests (Bourne *et al.*, 2015) and the proportion of seasonal E_i is within the range of other studies (Kergoat, 1998, Soubie *et al.*, 2016). Hence, it is not reasonable to believe that we largely underestimated E_t (by nearly 100%). A more plausible explanation is that we overestimated the effective rooting depth (Macinnis-Ng *et al.*, 2010), but without a detailed survey of root distribution we are unable to provide a more realistic φS. This latter explanation would agree with the estimates from a recent modelling study (Yang *et al.*, 2016a), which estimated an effective rooting depth of 1.2 m in the region. Here, we opted for a more conservative approach and established an effective rooting depth based our own observations and characterization of the soil texture profile. Nevertheless, despite the uncertainty regarding effective rooting depth, we found that eC_a had no effect on the temporal dynamics of S or φS at any depth during the entire study period, further supporting our argument that eC_a did not increased soil water-storage at any depth in this woodland.

In addition to our estimate of rooting depth, there may be other sources of uncertainty, such as our coarse approach to estimate R from measurements of P and soil properties. We established that R would only occur at times when the soil was fully saturated and precipitation exceeded the infiltration capacity, yet since EucFACE occurs on an alluvial floodplain, soil saturation may not occur homogeneously across the site. Indeed, some unquantified R might have been generated in areas where the soil saturated faster than the overall site mean due to spatial heterogeneity in soil texture. Furthermore, we did not account for the contribution of possible deep lateral flow that can occur in multilayered strongly contrasting textured soils (Cox & Pitman, 2002), such as at our site. These uncertainties could explain our inability to fully close the overall water balance for our study site for those seasons preceded by very rainy season, when we would have been more likely to underestimate D_g, R and lateral flow.

We examined the impact of eC_a on the hydrological balance of a native, mature woodland at the stand level for 30 months and during periods of water-limitation. Elevated C_a did not alter φS, E_{tree}, E_{floor}, E_i or E_t during this time Furthermore, eC_a did not indirectly affect E_t through changes in growth, phenology or L. In addition, we did not find significant effects of eC_a on the climatic forcing of transpiration, such that under a future climate change scenario (i.e. altered precipitation patterns and warmer global surface temperatures), more severe water-stress due to an increase in evaporative demand would not be alleviated under eC_a in this type of woodland. Based on this study, in water-limited catchments dominated by mature woodlands we should not expect changes in the amounts of precipitation partitioned to R and D_g in response to future increases in C_a.

Acknowledgements

Many thanks to Remko Duursma for his assistance with field data collection (leaf area index) and data analyses. Thanks also to Burhan Amiji, Craig Barton, Catherine Beattie, Vinod Kumar, Craig McNamara, Lindsay Nicks and Steven Wohl for their valuable contributions to our field work. We greatly acknowledge Margaret Barbour and Kevin Simonin for assistance in soil sample preparation for isotopic analysis at the University of Sydney; to David G. Williams and Craig Cook for sample processing and isotopic analyses at the University of Wyoming. Thanks to Belinda Medlyn and the ECOFUN team for constructive comments during manuscript preparation. EucFACE is supported by the Australian Commonwealth Government in collaboration with the Western Sydney University (WSU). EucFACE was built as an initiative of the Australian Government as part of the Nation-building Economic Stimulus Package. TEG was funded by a research collaborative agreement between CSIRO and WSU within the CSIRO Flagship program ôWater for a Healthy Countryô during this research, and funded by the IdEx programme of the Université de Bordeaux and a Marie Skğodowska-Curie Intra-European fellowship (Grant Agreement No. 653223) during manuscript preparation. Thanks to the three anonymous reviewers and the editor for comments that improved our original submission. All data used in the manuscript are stored in the institutional archive of the Western Sydney University and publicly available.

References

Aston AR (1984) The effect of doubling atmospheric CO_2 on streamflow - A simulation. Journal of Hydrology*,* **67**, 273-280.

Betts RA, Boucher O, Collins M *et al.* (2007) Projected increase in continental runoff due to plant responses to increasing carbon dioxide. Nature*,* **448**, 1037-U1035.

Bobich EG, Barron-Gafford GA, Rascher KG, Murthy R (2010) Effects of drought and changes in vapour pressure deficit on water relations of *Populus deltoides* growing in ambient and elevated CO_2. Tree Physiology*,* **30**, 866-875.

Bourne AE, Haigh AM, Ellsworth DS (2015) Stomatal sensitivity to vapour pressure deficit relates to climate of origin in *Eucalyptus* species. Tree Physiology*,* **35**, 266-278.

Campbell GS, Norman JM (1998) *An Introduction to Environmental Biophysics,* New York, Springer.

Cech PG, Pepin S, Körner C (2003) Elevated CO_2 reduces sap flux in mature deciduous forest trees. Oecologia*,* **137**, 258-268.

Cheng L, Zhang L, Wang Y-P *et al.* (2017) Recent increases in terrestrial carbon uptake at little cost to the water cycle. Nature Communications*,* **8**, 110.

Cheng L, Zhang L, Wang YP, Yu Q, Eamus D, O'Grady A (2014) Impacts of elevated CO_2, climate change and their interactions on water budgets in four different catchments in Australia. Journal of Hydrology, **519**, 1350-1361.

Collins L, Bradstock RA, Resco De Dios V, Duursma RA, Velasco S, Boer MM (2018) Understorey productivity in temperate grassy woodland responds to soil water availability but not to elevated [CO_2]. Global Change Biology, DOI: 10.1111/gcb.14038.

Cox JW, Pitman AJ (2002) The water balance of pastures in a South Australian catchment with sloping texture-contrast soils. In: *Regional Water and Soil Assessment for Managing Sustainable Agriculture in China and Australia.* (eds. McVicar TR, Rui L, Walker J, W. FR, L. C). Canberra, Australia, Australian Centre for International Agricultural Research.

Crockford RH, Richardson DP (2000) Partitioning of rainfall into throughfall, stemflow and interception: effect of forest type, ground cover and climate. Hydrological Processes, **14**, 2903-2920.

De Kauwe MG, Medlyn BE, Zaehle S *et al.* (2013) Forest water use and water use efficiency at elevated CO_2: a model-data intercomparison at two contrasting temperate forest FACE sites. Global Change Biology, **19**, 1759-1779.

Donohue RJ, McVicar TR, Roderick ML (2009) Climate-related trends in Australian vegetation cover as inferred from satellite observations, 1981-2006. Global Change Biology, **15**, 1025-1039.

Donohue RJ, McVicar TR, Roderick ML (2010) Assessing the ability of potential evaporation formulations to capture the dynamics in evaporative demand within a changing climate. Journal of Hydrology, 386, 186-197.

Donohue RJ, Roderick ML, McVicar TR, Farquhar GD (2013) Impact of CO_2 fertilization on maximum foliage cover across the globe's warm, arid environments. Geophysical Research Letters, **40**, 3031-3035.

Donohue RJ, Roderick ML, McVicar TR, Yang YT (2017) A simple hypothesis of how leaf and canopy-level transpiration and assimilation respond to elevated CO_2 reveals distinct response patterns between disturbed and undisturbed vegetation. Journal of Geophysical Research-Biogeosciences, **122**, 168-184.

Drake JE, Macdonald CA, Tjoelker MG *et al.* (2016) Short-term carbon cycling responses of a mature eucalypt woodland to gradual stepwise enrichment of atmospheric CO_2 concentration. Global Change Biology, **22**, 380-390.

Duursma RA, Barton CVM, Eamus D *et al.* (2011) Rooting depth explains CO_2 x drought interaction in *Eucalyptus saligna*. Tree Physiology, **31**, 922-931.

Duursma RA, Barton CVM, Lin YS *et al.* (2014) The peaked response of transpiration rate to vapour pressure deficit in field conditions can be explained by the temperature optimum of photosynthesis. Agricultural and Forest Meteorology, **189**, 2-10.

Duursma RA, Gimeno TE, Boer MM, Crous KY, Tjoelker MG, Ellsworth DS (2016) Canopy leaf area of a mature evergreen *Eucalyptus* woodland does not respond to elevated atmospheric CO_2 but tracks water availability. Global Change Biology, **22**, 1666-1676.

Ellsworth DS (1999) CO_2 enrichment in a maturing pine forest: are CO_2 exchange and water status in the canopy affected? Plant Cell and Environment, **22**, 461-472.

Ellsworth DS, Anderson IC, Crous KY *et al.* (2017) Elevated CO_2 does not increase eucalypt forest productivity on a low-phosphorus soil. Nature Climate Change, **7**, 279-282.

Ellsworth DS, Thomas R, Crous KY *et al.* (2012) Elevated CO_2 affects photosynthetic responses in canopy pine and subcanopy deciduous trees over 10 years: a synthesis from Duke FACE. Global Change Biology, **18**, 223-242.

Fatichi S, Leuzinger S, Paschalis A, Langley JA, Barraclough AD, Hovenden MJ (2016) Partitioning direct and indirect effects reveals the response of water-limited ecosystems to elevated CO_2. Proceedings of the National Academy of Sciences of the United States of America, **113**, 12757-12762.

Ferretti DF, Pendall E, Morgan JA, Nelson JA, Lecain D, Mosier AR (2003) Partitioning evapotranspiration fluxes from a Colorado grassland using stable isotopes: Seasonal variations and ecosystem implications of elevated atmospheric CO_2. Plant and Soil, **254**, 291-303.

Field CB, Jackson RB, Mooney HA (1995) Stomatal responses to increased CO_2 - Implications from the plant to the global scale. Plant Cell and Environment, **18**, 1214-1225.

Fisher JB, Melton F, Middleton E *et al.* (2017) The future of evapotranspiration: Global requirements for ecosystem functioning, carbon and climate feedbacks, agricultural management, and water resources. Water Resources Research, **53**, 2618-2626.

Gash JHC (1979) An analytical model of rainfall interception by forests. Quarterly Journal of the Royal Meteorological Society, **105**, 43-55.

Gedney N, Cox PM, Betts RA, Boucher O, Huntingford C, Stott PA (2006) Detection of a direct carbon dioxide effect in continental river runoff records. Nature, **439**, 835-838.

Gimeno TE, Crous KY, Cooke J, O'Grady AP, Ósvaldsson A, Medlyn BE, Ellsworth DS (2016) Conserved stomatal behaviour under elevated CO_2 and varying water availability in a mature woodland. Functional Ecology, **30**, 700-709.

Godbold D, Tullus A, Kupper P *et al.* (2014) Elevated atmospheric CO_2 and humidity delay leaf fall in Betula pendula, but not in *Alnus glutinosa* or *Populus tremula x tremuloides*. Annals of Forest Science, **71**, 831-842.

Gunderson CA, Sholtis JD, Wullschleger SD, Tissue DT, Hanson PJ, Norby RJ (2002) Environmental and stomatal control of photosynthetic enhancement in the canopy of a sweetgum (*Liquidambar styraciflua* L.) plantation during 3 years of CO_2 enrichment. Plant Cell and Environment, **25**, 379-393.

Huntington TG (2008) CO_2-induced suppression of transpiration cannot explain increasing runoff. Hydrological Processes, **22**, 311-314.

Jackson RB, Sala OE, Paruelo JM, Mooney HA (1998) Ecosystem water fluxes for two grasslands in elevated CO_2: a modeling analysis. Oecologia, **113**, 537-546.

Jarvis PG, Mcnaughton KG (1986) Stomatal control of transpiration ï Scaling up from leaf to region. Advances in Ecological Research, **15**, 1-49.

Keel SG, Pepin S, Leuzinger S, Körner C (2007) Stomatal conductance in mature deciduous forest trees exposed to elevated CO_2. Trees-Structure and Function, **21**, 151-159.

Keenan TF, Hollinger DY, Bohrer G, Dragoni D, Munger JW, Schmid HP, Richardson AD (2013) Increase in forest water-use efficiency as atmospheric carbon dioxide concentrations rise. Nature, **499**, 324-327.

Kelly JWG, Duursma RA, Atwell BJ, Tissue DT, Medlyn BE (2016) Drought x CO_2 interactions in trees: a test of the low-intercellular CO_2 concentration (C_i) mechanism. New Phytologist, **209**, 1600-1612.

Kergoat L (1998) A model for hydrological equilibrium of leaf area index on a global scale. Journal of Hydrology, **212**, 268-286.

Leuzinger S, Körner C (2007) Water savings in mature deciduous forest trees under elevated CO_2. Global Change Biology, **13**, 2498-2508.

Leuzinger S, Körner C (2010) Rainfall distribution is the main driver of runoff under future CO_2-concentration in a temperate deciduous forest. Global Change Biology, **16**, 246-254.

Macinnis-Ng CMO, Fuentes S, O'Grady AP *et al.* (2010) Root biomass distribution and soil properties of an open woodland on a duplex soil. Plant and Soil, **327**, 377-388.

Macinnis-Ng C, Zeppel M, Williams M, Eamus D (2011) Applying a SPA model to examine the impact of climate change on GPP of open woodlands and the potential for woody thickening. Ecohydrology, **4**, 379-393.

Marshall DC (1958) Measurement of sap flow in conifers by heat transport. Plant Physiology, **33**, 385-396.

McCarthy HR, Oren R, Finzi AC, Ellsworth DS, Kim HS, Johnsen KH, Millar B (2007) Temporal dynamics and spatial variability in the enhancement of canopy leaf area under elevated atmospheric CO_2. Global Change Biology, **13**, 2479-2497.

Morgan JA, Pataki DE, Körner C *et al.* (2004) Water relations in grassland and desert ecosystems exposed to elevated atmospheric CO_2. Oecologia, **140**, 11-25.

Nelson JA, Morgan JA, Lecain DR, Mosier A, Milchunas DG, Parton BA (2004) Elevated CO_2 increases soil moisture and enhances plant water relations in a long-term field study in semi-arid shortgrass steppe of Colorado. Plant and Soil, **259**, 169-179.

Nolan RH, Lane PNJ, Benyon RG, Bradstock RA, Mitchell PJ (2014) Changes in evapotranspiration following wildfire in resprouting eucalypt forests. Ecohydrology, **7**, 1363-1377.

Norby RJ, Delucia EH, Gielen B *et al.* (2005) Forest response to elevated CO_2 is conserved across a broad range of productivity. Proceedings of the National Academy of Sciences of the United States of America, **102**, 18052-18056.

Norby RJ, Sholtis JD, Gunderson CA, Jawdy SS (2003) Leaf dynamics of a deciduous forest canopy: no response to elevated CO_2. Oecologia*,* **136**, 574-584.

Nowak RS, Zitzer SF, Babcock D *et al.* (2004) Elevated atmospheric CO_2 does not conserve soil water in the Mojave desert. Ecology*,* **85**, 93-99.

Oren R, Phillips N, Katul G, Ewers BE, Pataki DE (1998) Scaling xylem sap flux and soil water balance and calculating variance: a method for partitioning water flux in forests. Annals of Forest Science*,* **55**, 191-216.

Paschalis A, Katul GG, Fatichi S, Palmroth S, Way D (2017) On the variability of the ecosystem response to elevated atmospheric CO_2 across spatial and temporal scales at the Duke Forest FACE experiment. Agricultural and Forest Meteorology*,* **232**, 367-383.

Pathare VS, Crous KY, Cooke J, Creek D, Ghannoum O, Ellsworth DS (2017) Water availability affects seasonal CO_2-induced photosynthetic enhancement in herbaceous species in a periodically dry woodland. Global Change Biology, DOI: 10.1111/gcb.13778.

Pfautsch S, Macfarlane C, Ebdon N, Meder R (2012) Assessing sapwood depth and wood properties in *Eucalyptus* and *Corymbia* spp. using visual methods and near infrared spectroscopy (NIR). Trees-Structure and Function*,* **26**, 963-974.

Porporato A, Daly E, Rodríguez-Iturbe I (2004) Soil water balance and ecosystem response to climate change. American Naturlalist, **164**, 625-632.

R Development Core Team R (2014) R: A Language and Environment for Statistical Computing.

Raz-Yaseef N, Rotenberg E, Yakir D (2010) Effects of spatial variations in soil evaporation caused by tree shading on water flux partitioning in a semi-arid pine forest. Agricultural and Forest Meteorology*,* **150**, 454-462.

Raz-Yaseef N, Yakir D, Schiller G, Cohen S (2012) Dynamics of evapotranspiration partitioning in a semi-arid forest as affected by temporal rainfall patterns. Agricultural and Forest Meteorology, **157**, 77-85.

Schäfer KVR, Oren R, Lai CT, Katul GG (2002) Hydrologic balance in an intact temperate forest ecosystem under ambient and elevated atmospheric CO_2 concentration. Global Change Biology, **8**, 895-911.

Schreiner-Mcgraw AP, Vivoni ER, Mascaro G, Franz TE (2016) Closing the water balance with cosmic-ray soil moisture measurements and assessing their relation to evapotranspiration in two semiarid watersheds. Hydrology and Earth System Sciences, **20**, 329-345.

Soubie R, Heinesch B, Granier A, Aubinet M, Vincke C (2016) Evapotranspiration assessment of a mixed temperate forest by four methods: Eddy covariance, soil water budget, analytical and model. Agricultural and Forest Meteorology, **228**, 191-204.

Swanson RH, Whitfield DWA (1981) A numerical analysis of heat pulse velocity theory and practice. Journal of Experimental Botany, **32**, 221-239.

Tor-ngern P, Oren R, Ward EJ, Palmroth S, McCarthy HR, Domec JC (2015) Increases in atmospheric CO_2 have little influence on transpiration of a temperate forest canopy. New Phytologist, **205**, 518-525.

Trancoso R, Larsen JR, McVicar TR, Phinn SR, Mcalpine CA (2017) CO_2-vegetation feedbacks and other climate changes implicated in reducing base flow. Geophysical Research Letters, **44**, 2310-2318.

Uddling J, Teclaw RM, Pregitzer KS, Ellsworth DS (2009) Leaf and canopy conductance in aspen and aspen-birch forests under free-air enrichment of carbon dioxide and ozone. Tree Physiology, **29**, 1367-1380.

Ukkola AM, Prentice IC, Keenan TF, Van Dijk AIJM, Viney NR, Myneni RB, Bi J (2016) Reduced streamflow in water-stressed climates consistent with CO_2 effects on vegetation. Nature Climate Change, **6**, 75-78.

Ward EJ, Oren R, Bell DM, Clark JS, McCarthy HR, Kim HS, Domec JC (2013) The effects of elevated CO_2 and nitrogen fertilization on stomatal conductance estimated from 11 years of scaled sap flux measurements at Duke FACE. Tree Physiology, **33**, 135-151.

Warren JM, Pötzelsberger E, Wullschleger SD, Thornton PE, Hasenauer H, Norby RJ (2011) Ecohydrologic impact of reduced stomatal conductance in forests exposed to elevated CO_2. Ecohydrology, **4**, 196-210.

Wood S (2006) *Generalized Additive Models: An Introduction with R*, Chapman & Hall/CRC.

Wullschleger SD, Norby RJ (2001) Sap velocity and canopy transpiration in a sweetgum stand exposed to free-air CO_2 enrichment (FACE). New Phytologist, **150**, 489-498.

Yang Y, Donohue RJ, McVicar TR (2016a) Global estimation of effective plant rooting depth: Implications for hydrological modeling. Water Resources Research, **52**, 8260-8276.

Yang YT, Donohue RJ, McVicar TR, Roderick ML, Beck HE (2016b) Long-term CO_2 fertilization increases vegetation productivity and has little effect on hydrological partitioning in tropical rainforests. Journal of Geophysical Research-Biogeosciences, **121**, 2125-2140.

Zhang L, Dawes WR, Walker GR (2001) Response of mean annual evapotranspiration to vegetation changes at catchment scale. Water Resources Research, **37**, 701-708.

Zhang Y, Peña-Arancibia JL, McVicar TR *et al.* (2016) Multi-decadal trends in global terrestrial evapotranspiration and its components. Scientific Reports, **6**, 19124.

Zhu Z, Piao S, Myneni RB *et al.* (2016) Greening of the Earth and its drivers. Nature Climate Change, **6**, 791-795.

Tables and Figures

Table 1. Total seasonal potential evapotranspiration (E_p), precipitation (P), surface runoff (R), drainage (D_g) change in soil water storage (φS) and total evapotranspiration (E_t). E_t is the sum of canopy interception (E_i), canopy transpiration (E_{tree}) and soil evaporation and understorey transpiration (E_{floor}). E_p, P, R and D_g were measured or calculated at the site level. Depicted values of φS, E_t, E_i, E_{tree} and E_{floor} are the mean (±se) of the three rings for each atmospheric CO_2 level (ambient, a, and elevated, e). There were no significant differences ($p > 0.01$) between CO_2 levels for any of the hydrological components. All values in mm per season.

Season	**CO_2**	**E_p**	**P**	**R**	**ΔS**	**E_t**	**E_i**	**E_{tree}**	**E_{floor}**
Spring-2012	a	429	92	0	-106±10	97±5	10±2	64±3	23±1
	e				-109±23	108±20	17±9	68±11	23±1
Summer-2013	a	486	377	31	133±17	190±22	47±9	109±15	35±2
	e				119±26	206±32	50±10	122±21	33±2
Autum-2013	a	296	155	0	-113±13	153±9	20±1	99±12	34±4
	e				-89±26	151±21	24±7	100±18	28±3
Winter-2013	a	197	84	0	-45±17	84±9	3±1	61±8	19±1
	e				-48±18	81±10	5±2	57±11	19±1
Spring-2013	a	488	250	0	114±40	120±13	21±8	75±6	24±1
	e				110±40	126±16	32±8	69±12	24±1
Summer-2014	a	536	151	0	-149±30	159±10	16±4	106±8	36±1
	e				-139±23	172±23	23±6	111±21	38±4
Autum-2014	a	275	170	0	-26±12	132±3	30±7	76±9	27±2
	e				-34±4	142±22	28±5	89±17	15±1
Winter-2014	a	195	150	0	25±3	80±6	18±1	50±6	13±0.2
	e				14±4	87±11	20±6	54±12	13±0.5

Table 2. Results (estimated coefficients ± se, *t* and *p*-value) of the best linear mixed model fit to canopy interception (E_i, log-transformed). Selected fixed factors were: event precipitation (P_{cum} in mm, log-transformed), event duration (in h) and leaf area index (L, in m^2 m^{-2}). The CO_2 treatment did not significantly affect E_i or the any of the effect sizes.

Fixed	**Estimate**	***t***	***p***
Log(P_{cumm})	0.322 ± 0.02	15.2	<0.001
Duration	0.03 ± 0.006	5.5	<0.001
L	-0.18 ± 0.09	-2.1	0.038

Table 3. Seasonal values of the ratio of precipitation (P) to potential evapotranspiration (E_p), P, surface runoff (R), drainage (D_g) change in soil water storage (φS) and total evapotranspiration (E_t). For terms measured at the ring level (φS and E_t), depicted values are the mean (se) of the six rings. The error denotes the disequilibrium from the closure of the water balanced calculated as: P ï R ï D_g ï φS ï E_t = 0. All values, except for P/E_p and |Error/P| (both unitless), are in mm per season.

Year	**2012**	**2013**				**2014**		
Season	**Spring**	**Summer**	**Autumn**	**Winter**	**Spring**	**Summer**	**Autumn**	**Winter**
P/E_p	0.21	0.78	0.53	0.42	0.51	0.28	0.62	0.77
P	92	377	155	84	250	151	170	150
R	0	31	0	0	0	0	0	0
D_g	19	6	-4	11	20	18	4	11
φS	-107 (11)	126 (14)	-101 (14)	-47 (11)	112 (25)	-144 (17)	-30 (6)	19 (3)
E_t	103 (9)	198 (18)	152 (10)	82 (6)	123 (9)	165 (12)	137 (10)	84 (6)
Error	78	16	108	37	-5	111	58	36
|Error/P|	0.84	0.04	0.69	0.44	0.02	0.74	0.34	0.24

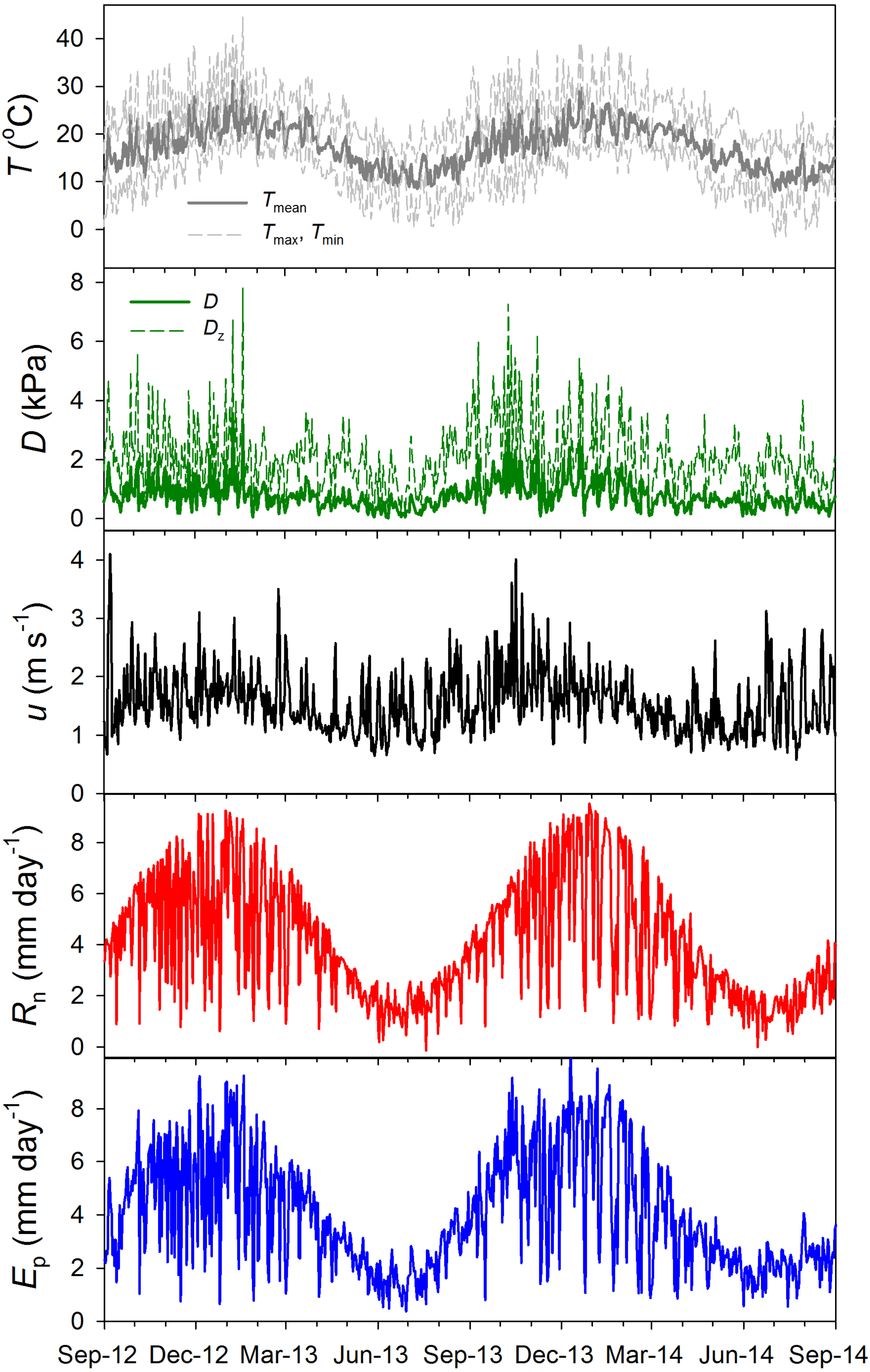

T (°C)
40
30
20
10
0
Tmean
Tmax, Tmin
D (kPa)
8
6
4
2
0
D
Dz
u (m s-1)
4
3
2
1
0
Rn (mm day-1)
8
6
4
2
0
Ep (mm day-1)
8
6
4
2
0
Sep-12
Dec-12
Mar-13
Jun-13
Sep-13
Dec-13
Mar-14
Jun-14
Sep-14

866

Fig. 1 Meteorological variables during the study period from top to bottom: maximum (T_{max}) and minimum (T_{min}) daily temperatures (dashed grey lines), mean daily temperature (T_{mean}), mean daily water pressure deficit (D, continuous green line) and day-length normalized D ($D_z = D\ n_d/24$, where n_d is the number of daylight hours dashed green line), mean daily wind speed (u), total net radiation (R_n) and total Penman potential evapotranspiration (E_p).

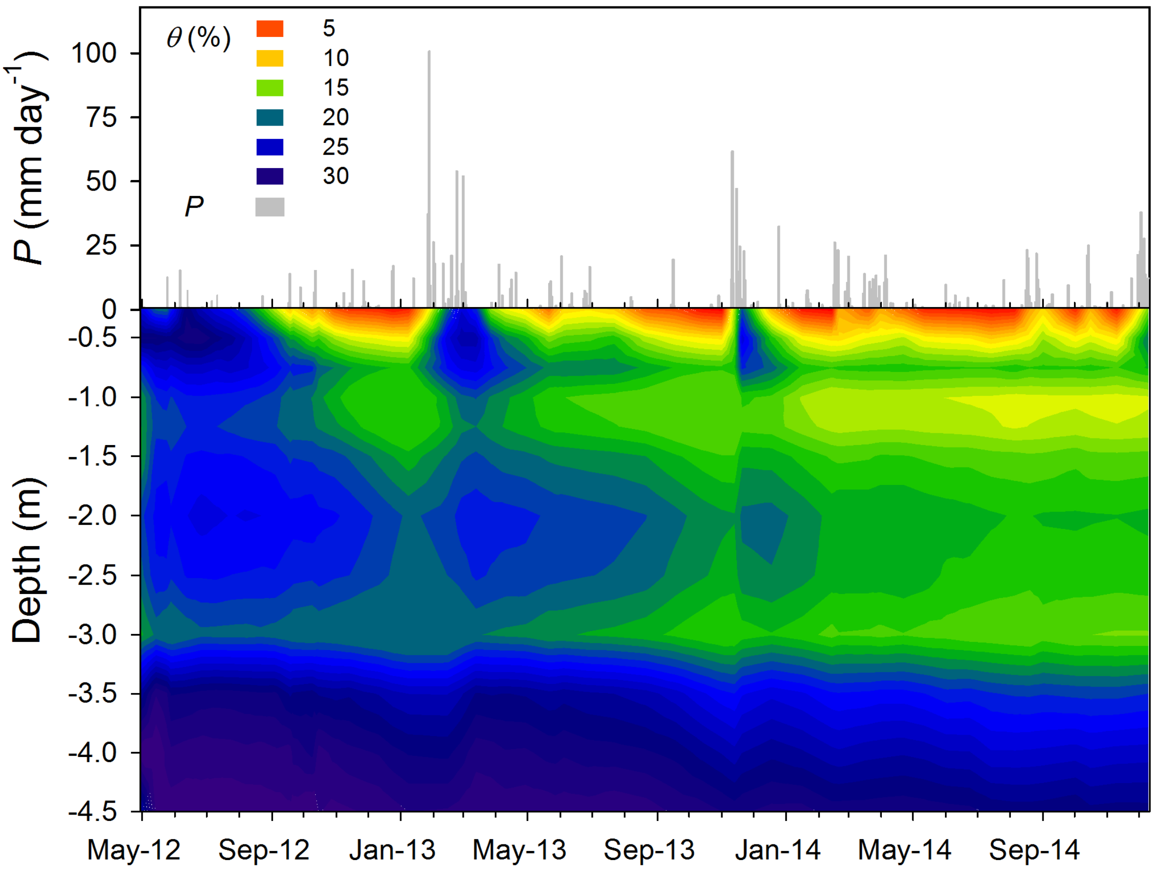

Fig. 2 Daily precipitation (*P*, grey bars) and temporal evolution of the vertical profile of soil volumetric water content (*θ*) inferred from mean (*n* = 6 rings) periodical measurements.

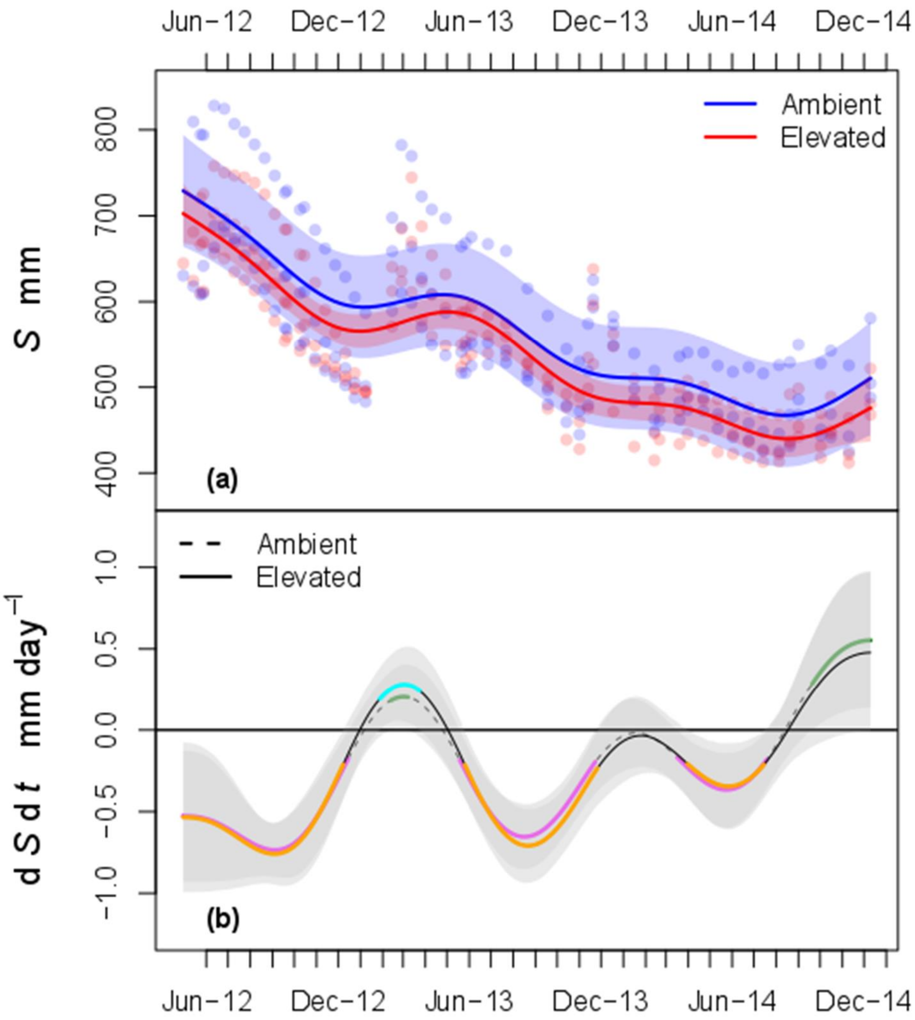

Fig. 3 (a) Soil water storage (*S*) over a soil column of 3 m depth, each point is the mean of two locations within each ring, lines and polygons represent the fitted generalized additive models with their 95% confidence intervals (CI) for each CO_2 treatment level. **(b)** Mean estimated daily changes in *S* (d*S*/d*t*, lines) and 95% CIs (polygons). Rates of change not significantly different from 0 are indicated with dashed (ambient) or continuous (elevated) black lines. Significantly negative changes are indicated with pink (ambient) and orange (elevated) lines and positive changes with cyan (elevated) and green (ambient) lines.

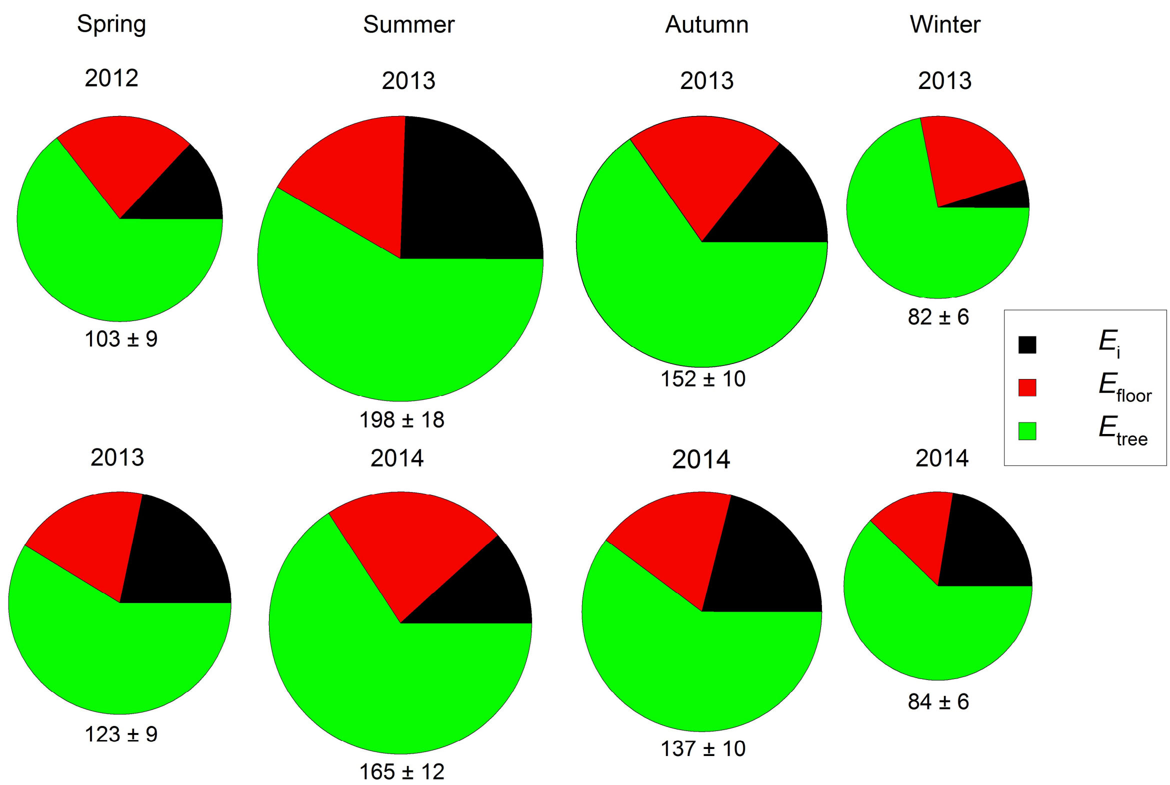

Fig. 4 Partitioning of total evapotranspiration among: canopy interception (E_i), canopy transpiration (E_{tree}) and understorey transpiration together with floor evaporation (E_{floor}). The size of each pie-chart is proportional to the corresponding seasonal evapotranspiration (in mm per season) indicated (site mean ± se, n = 6 rings).

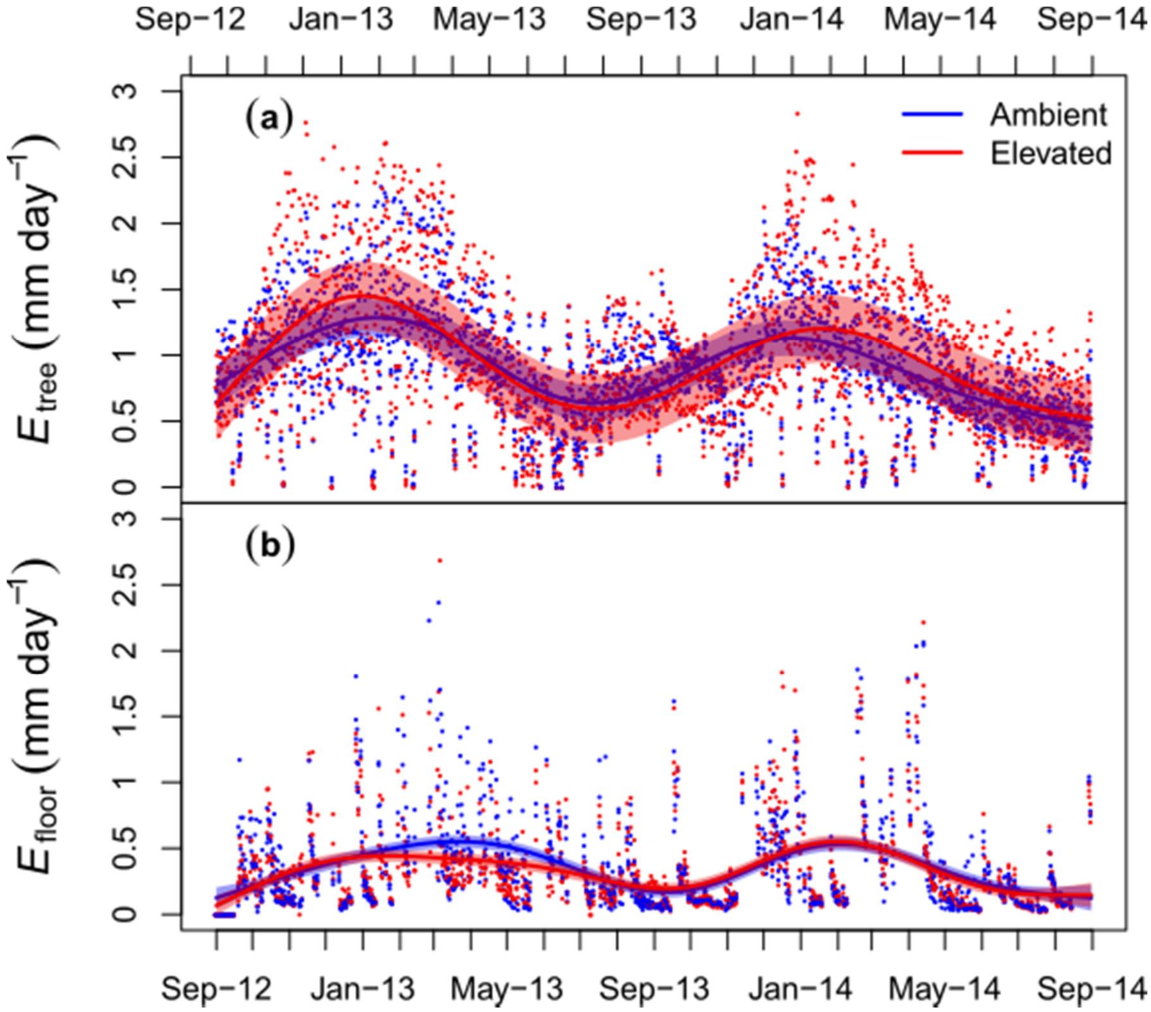

Fig. 5 **(a)** Estimated daily canopy tree transpiration (E_{tree}) and **(b)** understorey evapotranspiration (E_{floor}) for each ring under different C_a concentrations levels: ambient (blue) and elevated (red). Lines and polygons represent the fit of the GAMM for each C_a level with their 95% confidence intervals. E_{tree} was estimated from mean (n =3-4 trees per ring) sapflow velocities and E_{floor} was estimated from mean (n = 2 locations per ring) changes in shallow (5 cm) soil volumetric water content.

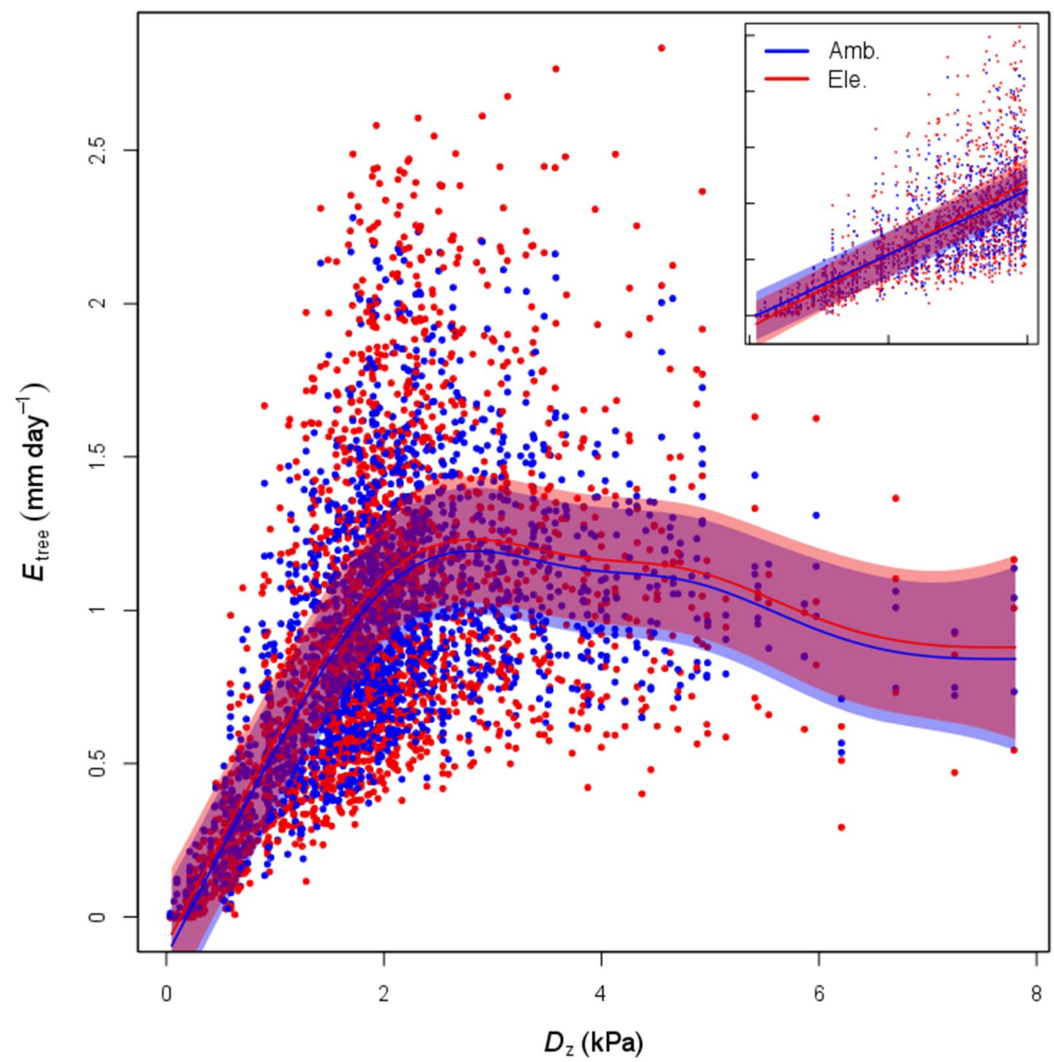

Fig. 6 Estimated daily canopy tree transpiration (E_{tree}) under different CO_2 concentrations: ambient (blue) and elevated (red) plotted against day-length normalised mean daily vapour pressure deficit (D_z). Lines and polygons represent the estimated fit of the GAMM for each CO_2 level with their 95% confidence intervals (CI). E_{tree} was estimated from mean (n =3-4 trees per ring) sapflow velocities. Figure inset represent the fits and CIs of a linear mixed model restricted to $D_z < 2$ kPa, where daily E_{tree} increased linearly with D_z ($t = 20.6$, $p < 0.01$) and depicted lines have slopes (±se) of 0.57 ± 0.03 and 0.67 ± 0.01 mm day^{-1} kPa^{-1}, for ambient and elevated CO_2 levels, respectively.